SCIENTIFIC REPORTS

OPEN

SUBJECT AREAS:
OPTICAL SPECTROSCOPY
CARBON NANOTUBES AND FULLERENES

Received
12 November 2014

Accepted
10 March 2015

Published
11 May 2015

Correspondence and requests for materials should be addressed to G.C. (giulio.cerullo@polimi.it) or G.L. (guglielmo.lanzani@iit.it)

High energetic excitons in carbon nanotubes directly probe charge-carriers

Giancarlo Soavi[1], Francesco Scotognella[1,2,3], Daniele Viola[1], Timo Hefner[4], Tobias Hertel[4], Giulio Cerullo[1,2] & Guglielmo Lanzani[1,3]

[1]Dipartimento di Fisica, Politecnico di Milano, Piazza L. da Vinci 32, 20133 Milano, Italy, [2]IFN-CNR, Piazza L. da Vinci, 32, 20133 Milano, Italy, [3]Center for Nano Science and Technology@PoliMi, Istituto Italiano di Tecnologia, Via Giovanni Pascoli, 70/3, 20133 Milano, Italy, [4]Inst. for Physical and Theoretical Chemistry Dept. of Chemistry and Pharmacy, University of Wuerzburg, Wuerzburg 97074, Germany.

Theory predicts peculiar features for excited-state dynamics in one dimension (1D) that are difficult to be observed experimentally. Single-walled carbon nanotubes (SWNTs) are an excellent approximation to 1D quantum confinement, due to their very high aspect ratio and low density of defects. Here we use ultrafast optical spectroscopy to probe photogenerated charge-carriers in (6,5) semiconducting SWNTs. We identify the transient energy shift of the highly polarizable S_{33} transition as a sensitive fingerprint of charge-carriers in SWNTs. By measuring the coherent phonon amplitude profile we obtain a precise estimate of the Stark-shift and discuss the binding energy of the S_{33} excitonic transition. From this, we infer that charge-carriers are formed instantaneously (<50 fs) even upon pumping the first exciton, S_{11}. The decay of the photogenerated charge-carrier population is well described by a model for geminate recombination in 1D.

The study of photo-excitation dynamics in one dimension has been prompted by theoretical predictions of a wealth of singular properties, such as the giant oscillator strength and non-linear response of confined states, the large Coulomb interaction, the sharply-peaked density of states and peculiar excited-state recombination kinetics[1–3]. In this respect, SWNTs represent a very close approximation to a 1D solid, easily achieving aspect ratio as high as 10^3. Theory predicts that Wannier-Mott excitons are the elementary photoexcitations in SWNTs, due to the strong Coulomb interaction caused by limited screening[4,5]. These excitons have typical 1D characteristics: negligible free carrier generation, large binding energy, non-negligible size and 1D transport. Theoretical predictions are supported by several experimental results, such as the measured binding energy, typically 0.1–1 eV[6,7], and the electron-hole correlation length, in the 2–5 nm range[8]. The exciton model alone, however, fails to capture the whole dynamics following photoexcitation, and many other photoexcited species have crowded the complex scenario of SWNTs' optical response, ranging from triplets[9] to bi-excitons[10] and trions[11]. Photocurrent[12–16], transient absorption[14,17,18] and THz spectroscopy[19,20] experiments also point out a non-negligible photogeneration of free charge-carriers in SWNTs. This is in stark contrast with the excitonic model and the reduced Sommerfeld factor that implies excitons be the only species generated upon photoexcitation. Attempts to solve this discrepancy proposed possible non-linear phenomena[21] as the mechanism of charge-carrier photogeneration in SWNTs. However, there is solid experimental evidence that the charge-carrier yield is linear with the pump fluence[19]. Besides this, the nature of high energetic transitions in small-diameter semiconducting SWNTs is still matter of debate, given that both excitonic[22,23] and band-to-band transitions[24,25] have been invoked to explain recent experimental results. Here we apply ultrafast optical spectroscopy to the semiconducting (6,5) SWNTs and show that charge-carriers can be identified by their effect on excitonic resonances, in particular the large energy shift that they induce on the third excitonic subband (S_{33}) transition. The availability of a good fingerprint for charge-carriers enables us to study their dynamics in one dimension. We find that, upon excitation of the lowest optical transition, a fraction of the absorbed photons generates geminate charge-carrier pairs "instantaneously" (<50 fs). The carriers recombine on the sub-nanosecond timescale following the characteristic kinetic law ($\sim t^{-1/2}$) of a random walk in 1D. This kinetics is consistent with an initial electron-hole separation of the same order as the exciton correlation length.

Results

Figure 1a shows the linear absorption spectrum of the sample with its first three excitonic transitions: S_{11} near 1 μm, S_{22} near 570 nm and S_{33} near 350 nm. Figure 1b shows $\Delta T/T$ spectra for 570 nm excitation wavelength at

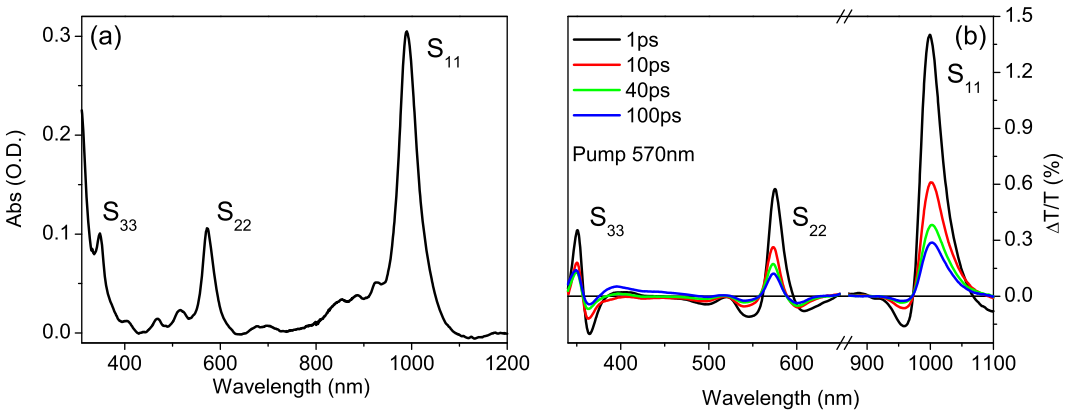

Figure 1 | Linear and transient absorption spectra of SWNTs. (a) Absorption spectrum of the enriched (6,5) SWNTs sample. (b) Transient absorption spectra at different pump-probe delays, with 570 nm excitation wavelength, for a (6,5) enriched SWNT sample. The probe is obtained with white light continuum, from CaF_2 for the wavelengths from 340 nm to 650 nm and from sapphire for wavelengths from 850 nm to 1100 nm.

different pump-probe delays. In agreement with our previous work[14], we find that the shape of the transient spectral response does not depend on the excitation wavelength (Supplementary material). We observe three sharp positive $\Delta T/T$ peaks corresponding to the three excitonic transitions, each associated with negative features, smaller than the positive one for the first and second excitons, but comparable for the third exciton. The large positive peak in the first exciton region can be assigned to photobleaching (PB) due to state filling. The photoinduced absorption (PA) above 1.1 μm has been tentatively assigned to triplets[26], metallic tubes[27], trions[21], transitions from S_{11} to the first band edge[28] or bi-excitons[29]. The complex shape of the $\Delta T/T$ signal around S_{22} can be reproduced with a red shift or a broadening of the ground state absorption spectrum. Several processes, such as photoinduced dephasing[30], bi-exciton formation[31,32], phonon dynamics[33] and charge induced Stark effect[14,18] have been invoked to explain the transient signal in this spectral region. Both the first and second excitons thus present complex transients, due to the superposition of several overlapping contributions. On the other hand, the third excitonic sub-band shows a simple first derivative lineshape that corresponds to a photoinduced red shift of the ground state transition.

Figure 2 zooms in on the transient $\Delta T/T$ spectra and dynamics in the region near S_{33} when the sample is excited at the S_{11} transition, with ≈50 fs temporal resolution (Fig. 2b). After rapid initial changes in the first ≈150 fs (Fig. 2a), the shape of the transient spectra remains unvaried up to 1 ns, the longest delay investigated here (inset of Fig. 2a). The observed derivative shape is insensitive to the pump-photon energy (Supplementary material), thus excluding bi-excitons and trions. Intensity dependent measurements (Fig. 2c and Supplementary information) demonstrate that the experiments, at least at lower fluences, are performed in a linear regime, thus ruling out non-linear processes such as two-photon absorption or exciton-exciton annihilation[21], which is expected to occur in a saturation regime for exciton photogeneration[34–36]. Similarly, the signal is weakly sensitive to changes in temperature (Supplementary material), excluding geometrical re-arrangement (i.e. diameter distortion) and thermal effects as a possible origin of the strong red-shift of S_{33} upon photoexcitation. In order to better understand the origin of the $\Delta T/T$ signal for S_{33}, we fit it by the sum of three contributions (Fig. 2d and Supplementary material): a Lorentzian function, corresponding to the ground-state PB, the difference between two Lorentzian functions, corresponding to a spectral red-shift by 0.13 eV, and a constant PA over the entire probe bandwidth. The ΔT/T signal for the third exciton is dominated by the spectral shift that we assign to the Stark shift induced on the S_{33} transition by the intense local electric field of photogenerated charge-carriers. The fit also indicates that PB, PA and Stark shift are all formed within our temporal resolution, as confirmed by the ultrafast build-up of the ΔT/T signal (Fig. 2b) and in good agreement with the claim of instantaneous charge photogeneration of Ref. 20. The PB signal decays faster (≈600 fs) with respect to the Stark signal, as expected for the lifetime of excitons with respect to free or trapped charge-carriers. The fast decay of the PB signal also suggests that at longer delays (i.e. few picoseconds to nanoseconds) the transient signal at the S_{33} transition directly probes charge-carriers. To obtain another precise estimate of the Stark shift of the S_{33} exciton we study the clear periodic temporal modulations of the ΔT/T signal around the S_{33} transition (Fig. 3a), that we assign to impulsively excited coherent phonons, namely the radial breathing modes (RBMs). Their coupling to the optical response of SWNTs can be easily understood: exciton binding energies are approximately inversely proportional to the tube diameter[37,38], so that the exciton absorption peak undergoes red or blue shift according to diameter variations. The resulting oscillations have zero amplitude at the peak of the resonance and maximum amplitude with opposite phase for higher and lower energies[39]. Figure 3b shows the oscillatory component of the $\Delta T/T$ signal for two wavelengths near the S_{33} peak. Fourier transform of the time traces indicates a dominant frequency of 318 cm^{-1} (Supplementary information), consistent with the RBM of the (6,5) SWNT. Figure 3a shows the corresponding amplitude and phase of the modulation versus probe energy. Interestingly, the peak resonance energy, indicated by the zero amplitude and by the phase jump (Fig. 3a), is red-shifted from the ground state S_{33} transition (at 349 nm). In other words, coherent RBM phonons modulate the Stark shifted transition, thus providing a very sensitive tool for measuring the Stark shift of the exciton resonance. We obtain $\Delta E_{Stark} \sim 130\ meV$, in excellent agreement with the results of the fitting model.

Discussion

The Stark effect depends on the transition's polarizability and is enhanced for excitons with small binding energy. In contrast to state filling which selectively affects only transitions involving populated states, the Stark effect lacks this selectivity and affects all optical transitions. Our assignment of a red-shift induced by Stark effect is based on the following chain of reasoning: i) charge-carriers are photogenerated in SWNTs; ii) each charge-carrier is a source of a strong local electric field; iii) the amplitude of the Stark signal has a distinct kinetics from that of the exciton PB, being in particular much longer lived; iv) any other source of modulation that could explain the first derivative shape of the ΔT/T spectra for S_{33} has been ruled out. We propose that photoexcitation at the S_{11} transition creates both excitons and free charge-carriers: the first bleaches S_{33} (due

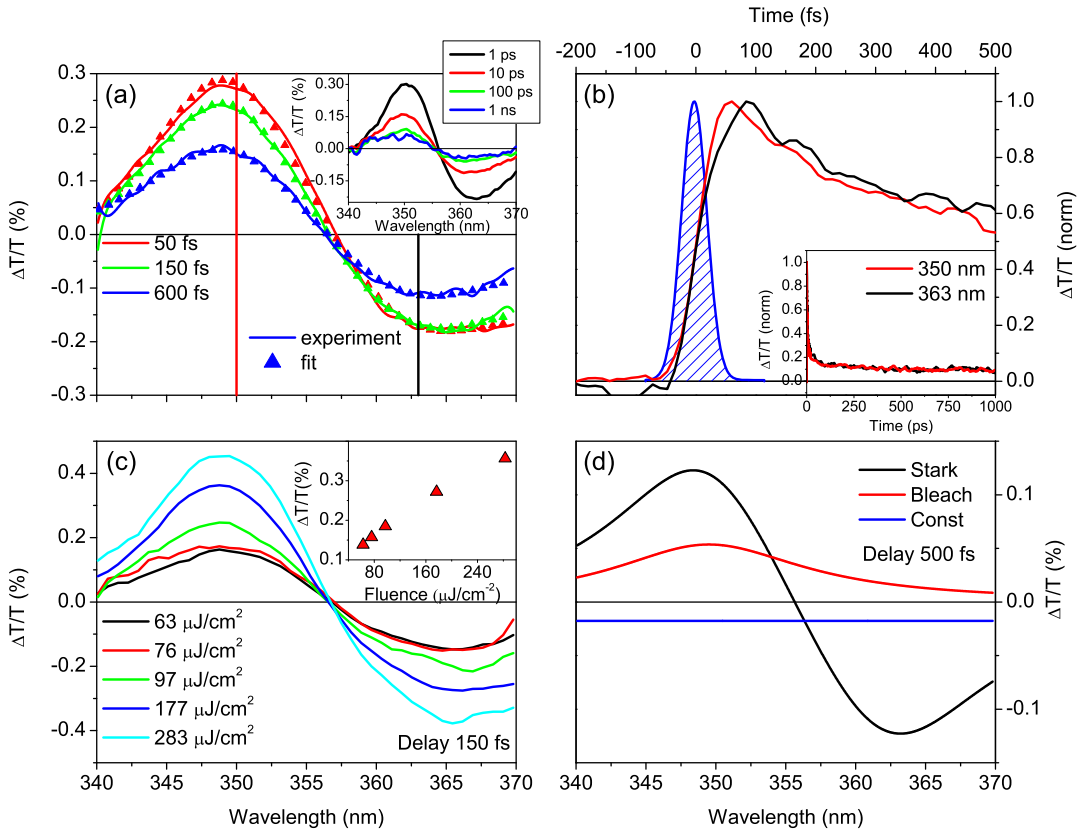

Figure 2 | (a) $\Delta T/T$ spectra at different pump-probe delays (solid line) and $\Delta T/T$ spectra obtained from the fitting (triangles). The excitation fluence is approximately 100 μJ/cm² for the main figure and 200 μJ/cm² for the inset. (b) Dynamics for wavelengths on the positive and negative peaks of the signal compared to our temporal resolution (≈50 fs). The pump pulse excites the first excitonic subband S_{11} in the IR region (≈1 μm). (c) Transient spectra at different pump intensities for 150-fs pump-probe delay and (inset) absolute value of the $\Delta T/T$ signal at 363 nm as a function of the pump fluence. (d) Spectral components used for the fitting, i.e. PB, PA and Stark shift, at 500 fs pump-probe delay.

ground state depletion and/or phase space filling), the latter shifts the energy levels due to Stark effect. The Stark effect prevails, making the S_{33} transition privileged to probe charge-carriers, for at least two reasons: i) the S_{33} exciton has small cross-section and thus small PB signal; ii) it has low binding energy[24,25], resulting in large field-induced energy shifts. The latter point deserves detailed attention. In fact, the nature of S_{33} in semiconducting SWNTs is still matter of debate: Rayleigh scattering experiments have demonstrated that it is consistent with an excitonic model[22], theoretical studies predict high binding energies[23] while recent experiments show features ascribable to unbound electron-hole pairs[24,25]. The PB contribution to the S_{33} transient signal (Fig. 2d) suggests that this transition is excitonic in nature and thus the quadratic part of the Stark effect can be expressed as $\delta E_{Stark} = \kappa_b^{(edF^2)}/E_b$, where κ_b is a fitting constant, e is the electron charge, d the SWNT diameter, F the electric field responsible for the Stark shift and E_b the exciton binding energy[40]. Since the Stark effect is inversely proportional to the exciton binding energy, we conclude that the large red shift (≈130 meV) that we observe on the S_{33} exciton is a consequence of its low binding energy (in agreement with Ref. 24), in particular if compared to lower-energy excitons (S_{11} and S_{22}), where the Stark shift is considerably smaller. In fact, the observation of a first derivative shape only for the highly polarizable S_{33} transition is readily accounted for by the Stark effect, while it could not be justified for other modulations that should affect all excitons in the same way.

Our data also give us the unique opportunity to analyze the dynamics of free charge-carriers in one dimension. Due to the linear dependence of the $\Delta T/T$ signal on pump fluence (inset Fig. 2c and Supplementary information), the most probable mechanisms of charge photogeneration remain either direct excitation or ultrafast linear exciton dissociation. According to our analysis, the charge-carrier population decay is monitored by the $\Delta T/T$ time trace at 363 nm, which represents the Stark amplitude evolution. Figure 3a shows that this decay is very accurately reproduced by a power law $(\Delta T/T)_{norm} = A \cdot t^{-1/2}$. The same power law is observed at different pump intensities (Supplementary material), thus excluding that the non-exponential kinetics is due to bimolecular non-geminate carrier annihilation. A monomolecular power law decay is the predicted dynamics for geminate recombination of free particles after random walk in an infinite one-dimensional chain[41]. In particular, the probability $\Omega(t)$ to survive at geminate recombination at delay t is expressed by $\Omega(t) = n_0 \Big/ \sqrt{2\pi W t}$, where W is the diffusion rate and $n_0 = L_0/a_0$ is the normalized initial particle separation, being L_0 the particle distance and a_0 the unit cell[41]. Considering that a hopping model is a good approximation for the high-mobility diffusive transport of SWNTs[42,43], we estimate the diffusion rate W as the inverse of the scattering time $\tau = m_{av}\mu/(0.32e)$, where m_{av} is the effective mass and μ is the charge-carrier mobility[44]. Using the value for mobility in a (6,5) SWNT of $\mu \sim 10^3\ cm^2/Vs$ (diameter of ≈1 nm)[44] and assuming $a_0 \sim 1\ nm$, we obtain $L_0 \sim 5\ nm$, meaning that the initial distance between a geminate electron-hole pair is of the same order of magnitude of the exciton correlation distance[8]. This suggests that "instantaneous" (<50 fs) linear exciton dissociation is the most likely mechanism of charge photogeneration. Possibly this process is favoured by the presence of atmospheric contamination, due to water and/or oxygen, which strongly reduces the exciton binding energy[45–49].

In conclusion, we identified the transient energy shift of the S_{33} transition as a sensitive fingerprint of charge-carriers in (6,5)

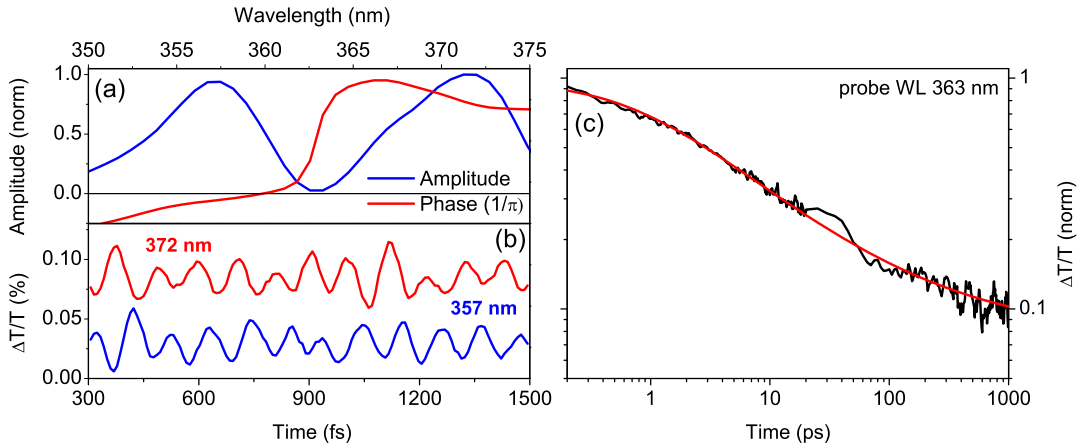

Figure 3 | (a) Fourier transform's amplitude and phase for the (6,5) RBMs' frequency (318 cm^{-1}) near the S_{33} energy region. (b) Oscillatory component at 357 nm (blue) and 372 nm (red), the two maxima of RBMs oscillations' amplitude. (c) Normalized dynamics at 363 nm (black) and fit (red) with a $A/\sqrt{t}$ function, where t is time and A is a fitting parameter. The excitation fluence is approximately 90 $\mu J/cm^2$.

SWNTs. The assignment is based on the notion that photogenerated charge-carriers give rise to strong electric fields that in turn shift the energy of the more polarisable transition, namely the S_{33} resonance. Modulation spectroscopy through coherent phonons allows a precise measurement of the Stark shift of the S_{33} exciton, from which we discuss its binding energy in comparison with lower energy excitonic transitions. Our results indicate that charge-carriers are formed even upon pumping the first exciton, S_{11}. This is a surprising outcome, since in principle S_{11} states are strongly bound and located well below the electron-hole continuum. The decay of the photogenerated charge-carrier population is well described by a model for geminate recombination in 1D. From the model, we estimate an initial charge-carrier separation of the same order of the exciton correlation length. This sheds additional light onto the generation mechanism, suggesting that the nascent excitons dissociate spontaneously, perhaps in presence of extrinsic screening of the Coulomb attraction due to water or other contamination. This result implies that charge photogeneration in SWNTs can be engineered, for instance for applications in optoelectronics, by manipulation of the tube environment. Long-lived charge carriers can only be obtained by promoting inter-tube separation, to escape efficient geminate recombination.

Methods

The sample used for these investigations is highly enriched in the (6,5) species and embedded in a gelatin film. This film was prepared from 30 microliters of a density gradient ultracentrifugation (DGU) enriched SWNT suspension in a sodium cholate (SC)/sodium dodecyl sulfate (SDS) mixture[50]. Iodixanol as well as SDS residues from the DGU process were removed by dilution with SC solution and filtration with a benchtop centrifuge. The resulting suspension with 30 microliters volume was then mixed with 20 microliters of 15 wt% gelatin solution and finally drop-cast on a thin glass substrate. Ultrafast pump-probe spectroscopy was carried out on a very broad wavelength region from 340 nm to 1.1 μm, thus probing the transient absorption signal of the third (S_{33}), second (S_{22}) and first (S_{11}) excitonic transitions of the sample (Fig. 1b). We excited the sample either with a broad IR pulse, peaked around 1 μm and with a transform-limited pulse duration of less than 15 fs (for measurements in Fig. 2 and 3) or with a 10-nm bandwidth pulse peaked at 570 nm (for measurements in Fig. 1b). As a probe we used: i) the second harmonic of a visible optical parametric amplifier (OPA), in order to achieve an overall temporal resolution of ≈50 fs in the probe region from 340 nm to 370 nm; ii) broadband white light super-continuum generated in CaF_2 in the probe region from 340 nm to 650 nm and iii) broadband white light super-continuum generated in a sapphire plate in the probe region from 850 nm to 1.1 μm. We measured the differential transmission ($\Delta T/T$) through the sample with an optical multichannel analyzer working at the full repetition rate (1 kHz) of the laser source[51].

1. Scholes, G. D. & Rumbles, G. Excitons in nanoscale systems. *Nat. Mater.* **5**, 683–696 (2006).
2. Scholes, G. D. Insights into excitons confined to nanoscale systems: electron-hole interaction, binding energy, and photodissociation. *ACS nano* **2**, 523–537 (2008).
3. Davies, J. H. *The physics of low-dimensional semiconductors* (Cambridge University Press: Cambridge, 1998).
4. Ando, T. Excitons in carbon nanotubes. *J. Phys. Soc. Jpn.* **66**, 1066–1073 (1997).
5. Ichida, M., Mizuno, S., Tani, Y., Saito, Y. & Nakamura, A. Exciton effects of optical transitions in single-wall carbon nanotubes. *J. Phys. Soc. Jpn.* **68**, 3131–3133 (1999).
6. Wang, F., Dukovic, G., Brus, L. E. & Heinz, T. F. The optical resonances in carbon nanotubes arise from excitons. *Science* **308**, 838–841 (2005).
7. Maultzsch, J. *et al.* Exciton binding energies in carbon nanotubes from two-photon photoluminescence. *Phys. Rev. B* **72**, 241402 (2005).
8. Lüer, L. *et al.* Size and mobility of excitons in (6, 5) carbon nanotubes. *Nat. Phys.* **5**, 54–58 (2008).
9. Stich, D. *et al.* Triplet–triplet exciton dynamics in single-walled carbon nanotubes. *Nat. Photonics* **8**, 139–144 (2013).
10. Pedersen, T. G., Pedersen, K., Cornean, H. D. & Duclos, P. Stability and signatures of biexcitons in carbon nanotubes. *Nano Lett.* **5**, 291–294 (2005).
11. Rønnow, T. F., Pedersen, T. G. & Cornean, H. D. Correlation and dimensional effects of trions in carbon nanotubes. *Phys. Rev. B* **81**, 205446 (2010).
12. Malapanis, A., Perebeinos, V., Sinha, D. P., Comfort, E. & Lee, J. U. Quantum Efficiency and Capture Cross Section of First and Second Excitonic Transitions of Single-Walled Carbon Nanotubes Measured through Photoconductivity. *Nano Lett.* **13**, 3531–3538 (2013).
13. Bindl, D. J. *et al.* Free Carrier Generation and Recombination in Polymer Wrapped Semiconducting Carbon Nanotube Films and Heterojunctions. *J. Phys. Chem. Lett.* **4**, 3550–3559 (2013).
14. Soavi, G. *et al.* Ultrafast Charge Photo-generation in Semiconducting Carbon Nanotubes. *J. Phys. Chem. C* **117**, 10849–10855 (2013).
15. Kumamoto, Y. *et al.* Spontaneous exciton dissociation in carbon nanotubes. *Phys. Rev. Lett.* **112**, 117401 (2013).
16. Barkelid, M., Steele, G. A. & Zwiller, V. Probing Optical Transitions in Individual Carbon Nanotubes Using Polarized Photocurrent Spectroscopy. *Nano Lett.* **12**, 5649–5653 (2012).
17. Gadermaier, C. *et al.* Long-lived charged states in single-walled carbon nanotubes. *Nano Lett.* **6**, 301–305 (2006).
18. Crochet, J. J. *et al.* Free-Carrier Generation in Aggregates of Single-Wall Carbon Nanotubes by Photoexcitation in the Ultraviolet Regime. *Phys. Rev. Lett.* **107**, 257402 (2011).
19. Beard, M. C., Blackburn, J. L. & Heben, M. J. Photogenerated free carrier dynamics in metal and semiconductor single-walled carbon nanotube films. *Nano Lett.* **8**, 4238–4242 (2008).
20. Jensen, S. A. *et al.* Ultrafast Photoconductivity of Graphene Nanoribbons and Carbon Nanotubes. *Nano Lett.* **13**, 5925–5930 (2013).
21. Santos, S. M. *et al.* All-optical trion generation in single-walled carbon nanotubes. *Phys. Rev. Lett.* **107**, 187401 (2011).
22. Berciaud, S. *et al.* Excitons and high-order optical transitions in individual carbon nanotubes: A Rayleigh scattering spectroscopy study. *Phys. Rev. B* **81**, 041414(R) (2010).
23. Spataru, C. D., Ismail-Beigi, S., Benedict, L. X. & Louie, S. G. Excitonic Effects and Optical Spectra of Single-Walled Carbon Nanotubes. *Phys. Rev. Lett.* **92**, 077402 (2004).
24. Araujo, P. T. *et al.* Third and fourth optical transitions in semiconducting carbon nanotubes. *Phys. Rev. Lett.* **98**, 067401 (2007).
25. Michel, T. *et al.* E_{33} and E_{44} optical transitions in semiconducting single-walled carbon nanotubes: Electron diffraction and Raman experiments. *Phys. Rev. B* **75**, 155432 (2007).

26. Park, J., Deria, P. & Therien, M. J. Dynamics and transient absorption spectral signatures of the single-wall carbon nanotube electronically excited triplet state. *J. Am. Chem. Soc.* **133**, 17156–17159 (2011).
27. Lüer, L. *et al.* Ultrafast dynamics in metallic and semiconducting carbon nanotubes. *Phys. Rev. B* **80**, 205411 (2009).
28. Ma, Y.-Z., Valkunas, L., Bachilo, S. M. & Fleming, G. R. Exciton binding energy in semiconducting single-walled carbon nanotubes. *J. Phys. Chem. B* **109**, 15671–15674 (2005).
29. Park, J., Deria, P., Olivier, J.-H. & Therien, M. J. Fluence-Dependent Singlet Exciton Dynamics in Length-Sorted Chirality-Enriched Single-Walled Carbon Nanotubes. *Nano Lett.* **14**, 504–511 (2014).
30. Ostojic, G. *et al.* Stability of high-density one-dimensional excitons in carbon nanotubes under high laser excitation. *Phys. Rev. Lett.* **94**, 097401 (2005).
31. Styers-Barnett, D. J. *et al.* Exciton Dynamics and Biexciton Formation in Single-Walled Carbon Nanotubes Studied with Femtosecond Transient Absorption Spectroscopy. *J. Phys. Chem. C* **112**, 4507–4516 (2008).
32. Gao, B., Hartland, G. V. & Huang, L. Transient Absorption Spectroscopy and Imaging of Individual Chirality-Assigned Single-Walled Carbon Nanotubes. *ACS nano* **6**, 5083–5090 (2012).
33. Koyama, T. *et al.* Transient Absorption Kinetics Associated with Higher Exciton States in Semiconducting Single-Walled Carbon Nanotubes: Relaxation of Excitons and Phonons. *J. Phys. Chem. C* **117**, 20289–20299 (2013).
34. Xiao, Y.-F., Nhan, T. Q., Wilson, M. W. B. & Fraser, J. M. Saturation of the Photoluminescence at Few-Exciton Levels in a Single-Walled Carbon Nanotube under Ultrafast Excitation. *Phys. Rev. Lett.* **104**, 017401 (2010).
35. Schneck, J. A. *et al.* Electron Correlation Effects on the Femtosecond Dephasing Dynamics of E_{22} Excitons in (6,5) Carbon Nanotubes. *J. Phys. Chem. A* **115**, 3917–3923 (2011).
36. Yuma, B. *et al.* Biexciton, single carrier, and trion generation dynamics in single-walled carbon nanotubes. *Phys. Rev. B* **87**, 205412 (2013).
37. Kataura, H. *et al.* Optical properties of single-wall carbon nanotubes. *Synth. Met.* **103**, 2555–2558 (1999).
38. Perebeinos, V., Tersoff, J. & Avouris, P. Scaling of excitons in carbon nanotubes. *Phys. Rev. Lett.* **92**, 257402 (2004).
39. Lim, Y.-S. *et al.* Coherent lattice vibrations in single-walled carbon nanotubes. *Nano Lett.* **6**, 2696–2700 (2006).
40. Perebeinos, V. & Avouris, P. Exciton Ionization, Franz−Keldysh, and Stark Effects in Carbon Nanotubes. *Nano Lett.* **7**, 609–613 (2007).
41. Zozulenko, I. V. Charge carrier geminate recombination in one-dimensional polymer structures with traps. *Solid State Commun.* **76**, 1035–1040 (1990).
42. Russo, R. *et al.* One-dimensional diffusion-limited relaxation of photoexcitations in suspensions of single-walled carbon nanotube. *Phys. Rev. B* **74**, 041405(R) (2006).
43. Bulmer, J. S. *et al.* Microwave Conductivity of Sorted CNT Assemblies. *Sci. Rep.* **4**, 3762 (2014).
44. Zhou, X., Park, J.-Y., Huang, S., Liu, J. & McEuen, P. Band Structure, Phonon Scattering, and the Performance Limit of Single-Walled Carbon Nanotube Transistors. *Phys. Rev. Lett.* **95**, 146805 (2005)
45. Lefebvre, J. & Finnie, P. Excited Excitonic States in Single-Walled Carbon Nanotubes. *Nano Lett.* **8**, 1890–1895 (2008).
46. Zhang, Q. *et al.* Plasmonic Nature of the Terahertz Conductivity Peak in Single-Wall Carbon Nanotubes. *Nano Lett.* **13**, 5991–5996 (2013).
47. Zahab, A., Spina, L., Poncharal, P. & Marlière, C. Water-vapor effect on the electrical conductivity of a single-walled carbon nanotube mat. *Phys. Rev. B* **62**, 10000–10003 (2000).
48. Kang, D., Park, N., Ko, J., Bae, E. & Park, W. Oxygen-induced p-type doping of a long individual single-walled carbon nanotube. *Nanotechnology* **16**, 1048 (2005).
49. Collins, P. G., Bradley, K., Ishigami, M. & Zettl, A. Extreme Oxygen Sensitivity of Electronic Properties of Carbon Nanotubes. *Science* **287**, 1801–1804 (2000).
50. Crochet, J., Clemens, M. & Hertel, T. Quantum Yield Heterogeneities of Aqueous Single-Wall Carbon Nanotube Suspensions. *J. Am. Chem. Soc.* **129**, 8058–8059 (2007).
51. Polli, D., Lüer, L. & Cerullo, G. High-time-resolution pump-probe system with broadband detection for the study of time-domain vibrational dynamics. *Rev. Sci. Intrum.* **78**, 103108 (2007).

Acknowledgments

C.G. acknowledges support by the EC under Graphene Flagship (contract no. CNECT-ICT-604391). F.S., G.L. and T.H. acknowledge the ITN project 316633 "POCAONTAS".

Author contributions

All authors discussed the results and implications and commented on the manuscript at all stages. G.S. and F.S. performed the pump-probe experiments, T.H. prepared the CNT sample, G.S. and D.V. performed the modelling of the pump-probe data. T.H. supervised the sample preparation, G.C. and G.L. supervised the pump-probe experiments and interpretation of the data.

Additional information

Supplementary information accompanies this paper at http://www.nature.com/scientificreports

Competing financial interests: The authors declare no competing financial interests.

How to cite this article: Soavi, G. *et al.* High energetic excitons in carbon nanotubes directly probe charge-carriers. *Sci. Rep.* **5**, 9681; DOI:10.1038/srep09681 (2015).